Preface

Piezoelectric materials (that includes all pyroelectrics and ferroelectrics) are used by industry in a very large range of applications. These include ultrasonic detectors, cleaners, imaging systems and sonar devices; ink-jet printer heads, diesel and gasoline fuel injectors for automobiles, trucks and vans; electronic memory devices such as Ferroelectric RAM; micro and nano positioning actuators, valves, motors, and translators; RF filters, resonators, and VCOs; among many other applications. There are many excellent books and reviews detailing the significance of this class of material - which can be polymer or ceramic; in bulk and thin film form; as 1D nano rods or wires to nanotubes and may also be processed as quantum dots. The properties of the materials have been shown, in some cases, to be dependent on their scale and dimension (as with many nanoscale material in fact) and perhaps, more importantly, the properties are highly non-linear with regards excitation voltage, mechanical stress and temperature. These factors make the development of measurement good practice and ultimately setting that down into documentary standards rather difficult.

In this book we are publishing, for the first time, a selection of NPL's Materials Measurement Good Practice guides and practically written reviews for the measurement of a large number of the important multifunctional parameters for a range of materials including ferroelectric bulk and thin films, piezoelectric actuators and sensors, pyroelectric devices, and electrostrictive materials. We first set out reminding ourselves the nature of polarisation in bulk materials and how this property is practically measured. We highlight some of the measurement pitfalls and common sources of error when you carry out the ubiquitous PE-loop measurement! Next we turn our attention to one of the standard measurement methods (available as an international standard in fact) for the evaluation of low field properties of piezoelectric ceramics, based on resonance analysis. A practical worked example takes the reader through the precise details of this test method and assists in the calculation of the materials properties. Another 'standard' test method, based on the original

ideas set out by Don Berlincourt back in the 1950's is presented in our next chapter and measurement good practice has been developed alongside one of the manufacturers of the test equipment. The results of an inter laboratory round robin are included in this chapter to show how the test method has been improved with regards accuracy of result. The pyroelectric properties of crystals (where a temperature change induces a polarisation in the material) are incredibly important for low light level thermal imaging cameras, motion detectors, people detectors and so on, and one of the leading experts in this field describes the details of how the tensor is measured accurately on a number of materials types in chapter . The use of interferometry to traceably measure the actuation displacement or strain of piezoelectric materials is next described using the double beam interferometric method. There are many additional details associated with the assessment of the materials properties of thin films which are not dealt with in this chapter, but are the subject of current intense research effort worldwide. The thermal properties of piezoelectrics often dominate high power use - such as in high power sonar or ultrasonic welding, for example. The particular issues with regards assessing the evaluation of the materials polarisation or strain characteristics at high temperatures is a complicated measurement problem which is explored in some detail in this chapter. An extension to the problems associated with self-heating (when a piezo transducer is electrically 'over-driven') in such high power applications is the subject of the next chapter and here we propose various ways in which the thermal properties of the transducer may be modelled using fairly simple methods. One of the more recent additions to the family of measurement methods for piezoelectrics (especially piezo thin films) is Piezoresponse Force Microscopy (PFM). Now, there are many excellent reviews published on this technique and indeed, the method is constantly evolving and new operational modes are being discovered every year. So, in this chapter we force ourselves to focus on the measurement apparatus and the principle mode of operation. Issues such as contact electro-mechanics and surface quality of the piezo film are evaluated and methods for quantifying the (to date) qualitative method are proposed. The mechanical properties of piezo thin films are of great importance in piezo-MEMS technology for example, and we devote a chapter to describe the operational principles behind an industry-standard mechanical indentation method for evaluating the elastic properties of piezo ceramics. The technique, on its own, is not sufficient to quantify all the elastic properties but, used with complementary methods such as SAW/ultrasonic propagation methods, it is a very useful tool that also allows for in situ electrical excitation of the piezo material. Finally, we spend some time discussing the measurement of dielectric breakdown in bulk piezoelectric ceramics based on the standards already developed for bulk electronic substrate dielectric materials. A final chapter on current standards (with links online) completes this volume.

The book is intended to occupy space in the research or technical lab where worked examples take the reader through some of the more tricky experi-

mental methods. This will be the first in a series of metrology volumes dedicated to the exploration of measurement good practice in piezoelectric and other multifunctional materials generally.

Teddington, *Markys Cain*
August 2013

Characterisation of Pyroelectric Materials

Professor Roger Whatmore

Department of Materials, Imperial College London, South Kensington Campus, Exhibition Rd, London SW7 2AZ, UK r.whatmore@imperial.ac.uk

1 Introduction

Pyroelectrics form a very broad class of materials. Any material which has a crystal structure possessing a polar point symmetry - i.e. one which both lacks a centre of symmetry and has a unique axis of symmetry - will possess an intrinsic, or spontaneous, polarisation and show the pyroelectric effect. The pyroelectric effect is a change in that spontaneous polarisation caused by a change in temperature. It is manifested as the appearance of free charge at the surfaces of the material, or a flow of current in an external circuit connected to it. The effect is a simple one, but it has been used in a range of sensing devices, most notably uncooled pyroelectric infra-red (PIR) sensors, and has thus come to be of some engineering and economic significance, enabling a wide range of sensing systems, ranging from burglar alarms through FTIR spectroscopic instruments to thermal imagers.

A wide range of material compositions and types are available for potential exploitation, including single crystals, ceramics, polymers, thin films and liquid crystals [1], [2]. An important problem for the materials engineer is how to select the most promising material for exploitation in any given device type. This must be determined by which of the materials properties are relevant to the application being contemplated. Central to the selection decision will be how to accurately measure these properties.

This chapter aims first to describe the main device applications of pyroelectrics and to discuss - on the basis of the physics of how these devices work - the key properties which determine device performance. It will then discuss the main techniques by which these properties can be measured, including some of the potential pitfalls. It will finish with a brief review of the properties of some of the materials which have been applied in practical devices and systems.

2 Basics of Pyroelectric Materials

As noted above, any material whose structure possesses one of the 10 polar symmetry groups (1, 2, m, mm2, 4, 4mm, 3, 3m, 6, 6mm) will be pyroelectric. The reasons for this are fairly simple to appreciate and are illustrated in Figure 1. This illustrates a very simple polar lattice in which a cation sits within an anion framework, but displaced from the centre of the unit cell (Figure 1a). This creates an intrinsic spontaneous electrical polarisation (P_S) to the cell. The cation sits in an asymmetric potential well (Figure 1b), which means that it will find it easier to move in one direction in the cell (back towards the cell centre) than the other. As the temperature of the material is increased, the amplitude of vibration of the cation will also increase, which means that its mean position will be closer to the centre of the cell, and thus the value of P_S will decrease with temperature. Simple examples of real materials which show the effect are ZnO and AlN, which both possess the wurtzite structure, symmetry 6mm [3]. In such materials, the magnitude of P_S decreases with increasing temperature but does not go to zero.

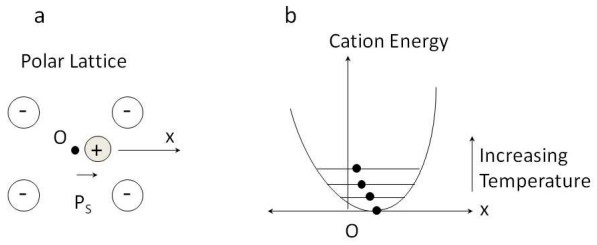

Fig. 1. Schematic diagram illustrating the origins of the pyroelectric effect. (a) Shows a cation sitting off-centre in a cation framework, generating a spontaneous electrical polarisation. (b) Shows the asymmetric potential well within which the cation sits.

The majority of pyroelectrics which have found practical applications belong to the class of materials known as ferroelectics [4]. In these materials, the direction of P_S can be switched between equivalent stable states by the application of an electric field of sufficient magnitude. This characteristic, known as ferroelectric hysteresis, is extremely useful, as it means that polycrystalline ferroelectric materials (ceramics and crystalline polymers) can be rendered polar, and hence pyroelectric through a process known as "poling". This usually entails cooling the material from a temperature close to (or even above) T_C while under a sufficiently-high electric field. The field orients the polar axes within the individual crystallites of the material so that they sum together to

give a net polarisation. Note that if there are a sufficient number of "options" for the polar axis within any one crystallite, the net polarisation can be close to that achieved in the bulk material (ca 80% for 6 or 8 options). Examples of ferroelectrics which have been used in pyroelectric applications include:

- $LiTaO_3$ which possesses the ilmenite structure, symmetry 3m at room temperature and for which the direction of P_S can be switched between two opposite directions. This is usually used in single crystal form.
- $PbTiO_3$, which possesses the perovskite structure, symmetry 4mm at room temperature and for which the direction of P_S can be switched between 6 equivalent directions. (In practical materials, this is usually modified with various other dopants, but the structure remains the same.) This is usually made and used as a polycrystalline ceramic.
- $Pb(Zr_{0.9}Ti_{0.1})O_3$, which also possesses the perovskite structure, but with symmetry 3m at room temperature and for which the direction of P_S can be switched between 8 equivalent directions. (Again, in practical materials, this is usually modified with various dopants.) This is also usually made and used as a polycrystalline ceramic.
- Poyvinylidene fluoride (PVDF) and its copolymers with trifluoroethylene. These are crystalline polymers with the symmetry mm2.

Several materials have been explored as polycrystalline thin films, usually deposited on silicon, in which the crystallites have a strongly-preferred orientation, which can enhance the pyroelectric effects. These materials will be discussed further below.

In nearly all ferroelectrics, the magnitude of P_S decreases with increasing temperature and goes to zero at the Curie temperature (T_C). In theory, the decrease in P_S is reversible, provided T_C is not exceeded but in practical applications, it is usual to operate the materials well below T_C, as usually P_S will degrade irreversibly unless a DC field is applied to stabilise it. This is discussed further below.

The change in P_S can be detected in the following way. If a piece of pyroelectric material is placed between electrodes, such that the vector P_S is normal to the electrodes and the electrodes are joined with a wire to make an external circuit (see Figure 2), then a change in temperature will cause a current ip to flow in the circuit such that:-

$$i_p = A\frac{dP_s}{dT} \cdot \frac{dT}{dt} \tag{1}$$

where: A = area of the electrodes
$\frac{dP_s}{dT}$ = Rate of change of P_S with temperature = p (pyroelectric coefficient)

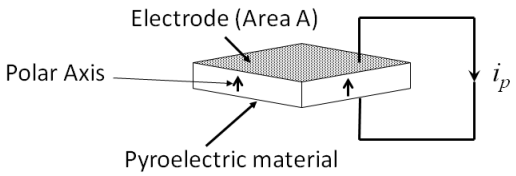

Fig. 2. Schematic diagram illustrating the generation of current by a pyroelectric element.

$\frac{dT}{dt}$ = Rate of change of temperature with time

This current flow can be used in a variety of ways, as will be illustrated in the next section. In ferroelectrics, the pyroelectric coefficient (p) will increase dramatically as T_C is approached, as shown schematically in Figure 3. However, there is a strong tendency for ferroelectrics to depole when close to T_C, even if T_C is not exceeded. Nevertheless, the polarisation - and hence the pyroelectric coefficient - can be stabilised close to, and even above, the T_C by the application of an electric field. In this case, the pyroelectric coefficient is given by *p(T,E)*:

$$p(T,\ E) = \frac{dD}{dT} \tag{2}$$

where D is the electrical displacement.

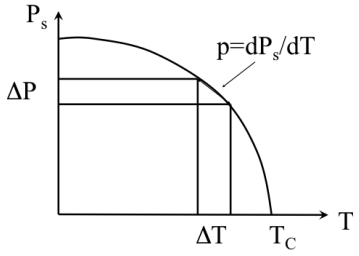

Fig. 3. Illustrating the variation of spontaneous polarisation with temperature in a ferroelectric exhibiting a second-order transition at the Curie temperature T_C.

This mode of operation, close to T_C with an applied electric field is frequently referred to as "dielectric bolometer mode". It has implications for the measurement of the physical properties which determine device operation, which will be discussed in more detail below.

It is important to note that the pyroelectric coefficient is a first rank tensor [5] and thus any crystalline material has a single major component, p.

3 Properties of Pyroelectrics for Radiation Sensing Applications

By far the most common application for pyroelectrics is the sensing of electromagnetic radiation. A typical device structure is shown schematically in Figure 4. Here, the pyroelectric is shown as thin piece, or element, which is electroded on its major faces. The wafer of the pyroelectric material is usually cut, or poled, so that the polar axis is perpendicular to the electrodes, but there are certain crystals for which an advantage can be gained by having the crystal cut so that p is not normal to the electrodes.

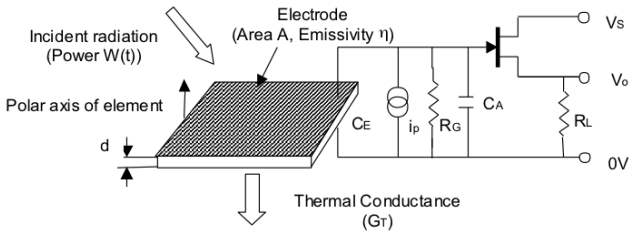

Fig. 4. Showing the structure of a typical pyroelectric detector.

The mode of operation is very simple. The radiation to be detected is allowed to fall on, and be absorbed by, the element - causing a change in element temperature. This causes a pyroelectric current i_p to flow through R_G, and a voltage to appear on the gate of the FET. (i_p is shown as a current generator symbol in Figure 4.) This modulates the transductance of the FET and hence produces an output voltage. Note that this amplifier configuration produces unity gain.

No discussion has yet been made of the wavelength of the radiation to be detected. This is because the detectors simply respond to the energy absorbed

from the radiation, and so can be used to detect any wavelength, provided there is sufficient energy present to give a detectable temperature change. Detectors have been demonstrated working at wavelengths from X-rays [6] to microwaves [7]. However, by far the most-common uses of pyroelectrics have been for detection of long-wavelength (8 to 12 micron) or mid-wavelength (3 to 5 micron) infra-red radiation (usually referred to as LWIR & MWIR respectively). This is because there are few other detectors which can give good performance at such wavelengths without the need for cooling. Resistive bolometers or thermopiles [8] can be used at room temperature, but semiconducting photon detectors generally require some cooling (usually to 77K for LWIR devices).

The radiation absorption can be achieved by coating the material with a suitable black coating. Examples include gold black [9], platinum black [10] or more-recently layers of carbon nanotubes [11]. Alternatively, the radiation can be absorbed in the material itself (in which case the front electrode should be arranged to be matched to the impedance of free space - 377Ω/square [12]. Other configurations which have been considered include the use of antenna coupling for microwaves or sub-millimetre waves [13].

Generally, pyroelectrics show adequate sensitivity for many LWIR applications, and the fact that they give an output proportional to rate-of-change of element temperature, and hence rate-of-change of radiation intensity, is an advantage in comparison with bolometers and thermopiles. The latter both give outputs proportional to element temperature, and hence radiation intensity. Thus pyroelectrics are very good for detecting the movement of warm (or cold) objects against a static, unchanging background scene, or for comparing radiation intensities from two different sources.

It is worth considering one further type of pyroelectric detector configuration. The detector configuration shown in Figure 4 has been widely applied in devices ranging from people sensors (burglar alarms, door openers, automatic light switches) to FTIR spectrometers and gas analysers. An example of a single element detector is shown in Figure 5. The device shown in Figure 4 works well at low frequencies (typically 0.1 to 100Hz) but, as will be shown below, the performance rolls-off rapidly at higher frequencies. This frequency response is determined by the thermal and electrical time constants (τ_T and τ_E) of the device. Nevertheless, there is nothing intrinsically "slow" about the pyroelectric effect itself, which is mediated by phonons in the material and can be in the picosecond range [14], [15]. Hence, very fast detectors can be made. These are usually edge-electroded, with the polarisation in the plane of the detector (Figure 6) so that the detector capacitance can be reduced and the device impedance matched to a 50 or 75W transmission line. The sensitivity of such detectors is generally very low, but in applications such as the characterisation of very fast, high power laser pulses, this is not usually a

problem. In this case the lack of a front electrode eliminates the possibility of it being damaged by the pulse.

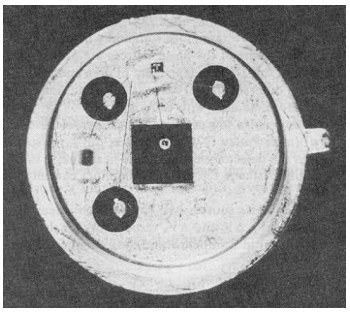

Fig. 5. Photograph of a single-element pyroelectric detector. The element is the black square in the centre of the package, the FET is the component immediately above it and the gate bias resistor is the component on the left.

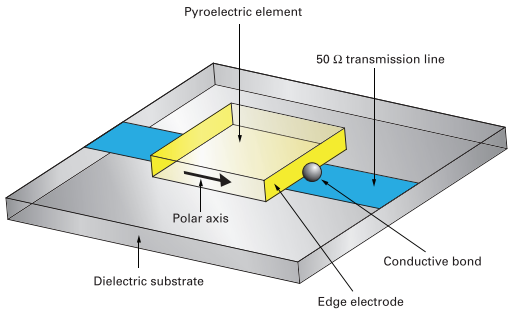

Fig. 6. Diagram of an edge-electroded pyroelectric detector.

The physics of operation of the device shown in Figure 4 has been extensively discussed elsewhere [1], [16], [17], [18]. It can be shown that, for radiation of intensity W_0 and modulated at frequency ω, the pyroelectric current i_p, generated per watt of input power (the current responsivity R_iRi) is given by:

$$\frac{i_p}{W_0} = R_i = \frac{\eta p A \omega}{G_T(1+\omega^2\tau_T^2)^{1/2}} \tag{3}$$

The form of this response is simple. At low frequencies ($\omega \ll 1/\tau_T$) the response is proportional to ω. For frequencies much greater than $1/\tau_T$ the response is constant, being:

$$R_i = \frac{\eta p A}{H} = \frac{\eta p}{c' d} \tag{4}$$

where $c^{'}$ is the volume specific heat.

Equation 4 gives us the first 'figure-of-merit' which relates the fundamental physical properties of the pyroelectric material with the current responsivity of the device. This is:

$$F_i = \frac{p}{c'} \tag{5}$$

In this case, we should choose materials with high values of p and low values of c' to maximise the current responsivity.

The voltage responsivity of the detector can be derived from the pyroelectric current i_p and the complex electrical admittance presented to it. The pyroelectric voltage (V_p) generated on the gate of the FET, and therefore the output voltage V_o for a unity amplifier gain and the voltage responsivity (R_V) where:

$$R_V = \frac{i_p}{YW_0} = \frac{R_G \eta p A \omega}{G_T (1 + \omega^2 \tau_T^2)^{1/2} (1 + \omega^2 \tau_E^2)^{1/2}} \tag{6}$$

This function peaks at a frequency $\omega_{peak} = (\tau_E \tau_T)^{-1/2}$, with a value:

$$R_V(max) = \eta p A \frac{R_G}{G_T} \frac{1}{(\tau_E + \tau_T)} \tag{7}$$

The variation of R_V with frequency is shown in Figure 7, in this case for a 100 micron square, 25 micron thick ceramic detector element feeding into a typical MOSFET amplifier and with a thermal conductance of 20mW/K.

Between the two frequencies τ_E^{-1} and τ_T^{-1}, the value of R_V varies by no more than a factor of $\sqrt{2}$ less than R_V(max). Below the lower of these two frequencies, R_V increases as ω^{-1} and above the greater of the two, R_V decreases as ω^{-1}. In the latter region, at high frequencies and for device designs where the element capacitance C_E dominates in Figure 4, the voltage responsivity is given by:

$$R_V = \frac{\eta p}{c' \epsilon \epsilon_0 A \omega} \tag{8}$$

This gives us the second figure-of-merit, F_V, where:

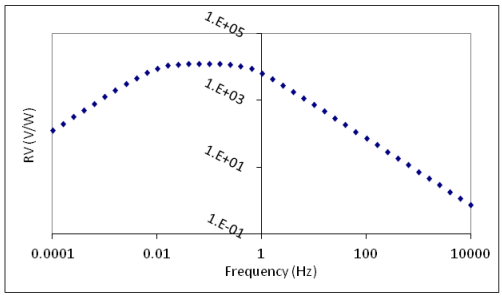

Fig. 7. R_V vs frequency for a pyroelectric ceramic element with area 1mm^2 and thickness 50 microns, and thermal conductance to the substrate of 50μW/K.

$$F_V = \frac{p}{c'\epsilon\epsilon_0} \tag{9}$$

This is frequently seen in the literature as the most-important figure-of-merit for pyroelectric detectors. However, it should be noted that for most situations, the devices are designed and operated at a frequency to maximise the value of R_V, which is given by Equation 7. Furthermore, C_E may not dominate over C_A. In this case there is no simple relationship between the material's properties and the voltage responsivity which can be used to give a simple 'figure-of-merit' describing the device's performance, and it is necessary to model the performance of the various available materials in the device structure, and optimise the design accordingly. However, maximising the value of F_V is generally a good idea, but it is important to take note of the following points:

- For very small element detectors, where the capacitance of the amplifier may be significantly greater than that of the element, F_i is likely to be the most-useful figure-of-merit. In other words, it may be more useful to maximise p than the ratio p/ϵ. Small detector elements are important for thermal imaging and other array applications, when it is necessary to have a large number of elements in a finite area, defined by read-out IC and optical system implications. Such elements can be as small as 40 microns across [16].
- In general, the best performance will be obtained if the capacitance of the detector element at least matches that of the amplifier. Hence, for small detector elements it can be important to have a high dielectric constant for the pyroelectric material.
- The appearance of G_T in the denominator of Equation 7 means that the thermal conductivity (k) of the pyroelectric material can be important in determining R_V, although this depends upon the thermal structure of the

device. Generally, the thermal diffusivity ($\kappa = k/c'$) is as important as the value of k.

Finally, the importance of noise in a sensor cannot be ignored. There are several sources of noise in a pyroelectric detector [1], [16], [17], including the thermal fluctuation noise (usually negligible), the voltage and current noise in the amplifier, the Johnson noise in the gate bias resistor (which can include a component due to the DC leakage in the pyroelectric material) and the dielectric noise in the pyroelectric. The latter two components usually dominate. In particular, the dielectric noise is proportional to $(\omega\epsilon\epsilon_0 \tan\delta)^{1/2}$, and it is often useful to define a figure of merit which determines the specific detectivity (D*) of the detector:

$$F_D = \frac{p}{c'\sqrt{\epsilon\epsilon_0 \tan\delta}} \tag{10}$$

Finally, all pyroelectrics are piezoelectric - they will generate charge under mechanical stress. This has two consequences:
Firstly, the pyroelectric coefficient (p^{stress}) which we normally measure under constant (ideally zero) stress consists of two components, a primary component which we would measure at constant strain (p^{strain}) - a 'clamped' value - together with a secondary component (p^{sec}) which emerges through a combination of the thermal expansion coefficients of the film (α_{ij}) coupling to the piezoelectric coefficients (e_{ijk}). It is easy to show that:

$$p_3^{stress} = p_3^{strain} + e_{ijk}\alpha_{jk} \tag{11}$$

Where the normal repeated suffix summation convention has been used for the tensor coefficients. Generally, the primary coefficient values at constant strain are not important, but the coupling of a pyroelectric thin film to a substrate which has a different thermal expansion coefficient from the film can make a significant difference to the apparent pyroelectric effect (up to $\pm 50\mu Cm^{-2}K^{-1}$ - [19]), depending on the relative values of the thermal expansion coefficients of film and substrate and the piezoelectric coefficients of the films. This can make a difference of up to 20% to the measured values. Generally, the most important of the piezoelectric coefficients to know in determining the magnitude of this effect is e_{31} or $d_{31}/(s_{11} + s_{12})$ [20].

Secondly, from a device performance point-of-view, the piezoelectric effects can be a source of significant electrical noise in a mechanically-noisy environment [21]. This effect is generally termed piezoelectric 'microphony'. Its effects can be minimised by good device and packaging design. However, in order to do this it is again important to know the value of d_{31}, as the largest contribution to the effect comes from the flexure of the substrate to which the element is mechanically connected. The contribution due to self-loading through the

thickness of the element (for which the coefficient d_{33} would provide the coupling) is generally small.

Hence, in summary, the material properties which it is important to measure for pyroelectric detector device design are as follows:

- The constant-stress pyroelectric coefficient, p. For ceramic and polymeric materials, it is sufficient to know the magnitude of this quantity, as the principal axis direction will always be parallel to the poling direction, but for single crystals, it is important to know the orientation of this with respect to the crystallographic axes.
- The real and imaginary parts of the dielectric permittivities of the material (e'_{ij} and e''_{ij}). As dielectric permittivity is a second-rank tensor, all the major axis components are needed, together with their orientations with respect to the crystallographic axes. These are essential if a crystal cut is to be used which is not perpendicular to the major axis of the pyroelectric coefficient. The imaginary parts of the dielectric permittivities are also needed to determine the relevant loss tangent, and hence f_D. Dielectric properties (especially loss tangents) are strongly dependent on frequency, and so it is essential to determine these properties at the frequency at which the device will be operated.
- Electrical resistivity (ρ). This will determine the electrical leakage in the device. With care over control of the electrical properties, especially resistivity, the bias resistor r_G shown in Figure 4 can be "built in" to the material and eliminated as an external component [22], [23], [24].
- Volume Specific Heat (c'). This is the product of the mass specific heat (c_p) and the density.
- Thermal Conductivity (k) and Thermal Diffusivity (κ). These will determine the thermal conductance of the device, and hence the thermal time constant. For array-based devices in which there is no separation of adjacent elements, the thermal diffusivity will determine the degree of thermal crosstalk between adjacent elements.
- The piezoelectric coefficients (e_{ij}, d_{ij}) are important in determining secondary pyroelectric effects and the level of piezoelectric microphony. e_{31} and d_{31} are the most significant parameters to determine for pyroelectric applications.
- Optical properties: The refractive index and optical loss at the wavelength to be sensed can be important if the absorption of the electromagnetic radiation is to be in the element itself.

4 Measurement of Physical Properties

4.1 Sample Poling

The majority of materials of-interest for pyroelectric applications are ferroelectric, and therefore all the properties should be measured with the material in the poled state. A wide variety of methods have been used to pole ferroelectric materials [4], and for each material it is necessary to determine the optimum poling conditions before definitive property measurements are done. Some of the methods which can be used include:

- Slow cooling of the specimen under a field which is usually a multiple of the coercive field. The specimen is generally held in a bath of an insulating fluid such as a silicone or mineral oil. This is to minimise the risk of surface breakdown and electrical shorting. This method is widely applied to ferroelectric ceramics used for piezoelectric and pyroelectric applications. For example, a modified lead zirconate [25] with a T_C of 230°C and a value for E_c of ca 10KV/cm could be reliably poled by cooling from 150°C to room temperature under a field of 30KV/cm over a period of ca 30 mins. Similar conditions can be used to pole pyroelectric thin films based on a $Pb(Zr_{0.3}Ti_{0.7})O_3$ composition.
- Materials with very high values of T_C (e.g. $LiTaO_3$, T_C ca 620°C) are often too electrically conductive to pole using the above method - it leads to electrical breakdown. One technique which can be used in this instance is to slow cool the material through T_C with a pulsed field applied [26]. The field and the duty cycle need to be optimised for the individual material.
- Corona poling [27] is a technique which has been successfully applied to polymeric ferroelectrics such as PVDF. It consists of exposing one, non-electroded, face of the ferroelectric to a corona discharge from a series of metal points held at high voltage (typically >10KV). The back face of the material is earthed. It has the advantage that, as there is no front electrode, the risks of catastrophic breakdown through a physical defect in the film are much reduced. Recently, it has been demonstrated that this technique can be successfully used for poling ferroelectric thin films [28].

4.2 Pyroelectric coefficient

Several techniques have been employed for measurement of the pyroelectric coefficient. These are reviewed and discussed below.

Charge Integration

Probably the simplest technique is to heat the material, and integrate the pyroelectric current using a standard charge-integrator circuit, employing a

good-quality, FET-input op-amp. An example of such a circuit is shown in Figure 8. This is the method described by Lang and Steckle [29] and Glass [30]. The FET input is important to give a high input impedance (R_i), which will then give a long integration time-constant (C_i). The charge-integrating capacitor should be sufficiently-large so that the time constant R_iC_i is much greater than the length of time to make the experiment. For $R_i = 10^{12}\Omega$ and C_i=10μF, the time constant would be amply long enough >100 days. The choice of the integrating capacitor is important, as it is essential to minimise leakage. A good quality polyester variety is a good choice, rather than ceramic or electrolytic. If a sample of a typical pyroelectric material is considered (say $LiTaO_3$ - see below - for which p=200x10^{-6} $Cm^{-2}K^{-1}$), with an area of 1cm^2, this value of capacitor would give an integration output in the millivolt range for every degree centigrade change in temperature. This can easily be measured using an appropriate digital voltmeter. The sample temperature can be measured using a thermocouple placed close to the specimen. A Chromel/Alumel thermocouple will produce an output voltage change of approximately 40 micovolts per °C, although this is temperature dependent and the appropriate calibration curve must be used. The thermocouple voltage can also be measured using a DVM, or with an appropriate digital thermometer. Other devices can be used to measure temperature, such as a Pt resistance thermometer or commercial thermistor. The integrated charge can be logged as a function of temperature, to produce charge integration curves on heating and cooling.

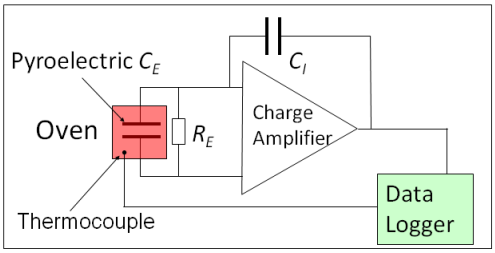

Fig. 8. Charge integration circuit.

The pyroelectric coefficient at any given temperature can be simply determined from the gradient $\frac{dQ}{dT}$ of this curve and the electrode area (A).

$$p = \frac{dQ}{dT} \cdot \frac{1}{A} \tag{12}$$

Key issues in making this measurement are:

- As in all temperature measurement, the thermocouple (or other device) must always be at the same temperature as the material being measured. Hence, the design of the heating system is important. Placing the sample on, or within, a large thermal mass within the oven, such as a brass block, can be effective. The thermal mass of the block ensures that the heating and cooling cycles are smooth and steady. The location of the thermocouple in the block, close to the pyroelectric sample being measured, ensures that the measured temperature is as close as possible to the actual temperature of the sample. The sample should be contained within an electrically shielded environment, which reduces the electrical noise. The leads connecting the sample to the charge integrating amplifier should also be fully and individually shielded, with the shields earthed, which reduces stray capacitance (important if the rig is to be used for dielectric measurements see below) and keeps electrical noise to a minimum. If required, channels can be machined into the heating/cooling block to allow the circulation of a coolant fluid. If a measurement below ambient temperature is required, the sample oven must be filled with dry gas (with a dew point below the lowest temperature to be used, or evacuated, to prevent the condensation of moisture onto the specimen).
- The measurement of pyroelectric currents can easily be confused by the release of trapped charges, causing thermally-stimulated currents (TSC). The trapped charges are usually caused by the separation of mobile charge during poling, which become trapped in lattice or structural defects, grain boundaries, electrode interfaces etc. The effect of TSCs is to increase the current released on heating, and reduce it on cooling, so that the gradients of the charge integration curves are greater on heating and reduced on the cooling cycle. The best way to avoid this effect is to wait for a decent length of time (typically 24 hours) after poling, before making the pyroelectric measurement. Annealing the sample in an oven for several hours, with the electrodes shorted, can also help to reduce this effect. Clearly the annealing temperature should be well below the Curie temperature. For a typical modified lead zirconate ceramic referred to above, an overnight anneal at 100°C is usually found to be effective. In any case, it is important to take the pyroelectric coefficients both on heating and on cooling and any residual TSCs taken account of. This can be done as described below.

Pyroelectric Current Measurement

The use of this method has been described by Byer and Roundy [31] and consists of heating or cooling the sample at a known rate while measuring the pyroelectric current - either using a commercial electrometer or using a circuit of the type shown in Figure 9. The currents can be very small - of the

order of nanoamps or less. Hence the circuit needs to be sensitive and well-shielded from sources of electrical noise. There are many excellent examples of commercial devices capable of measuring very low currents.

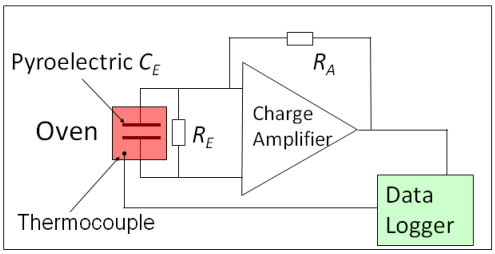

Fig. 9. Circuit for measurement of pyroelectric currents.

Figure 10(a) shows an example of results obtained from this type of measurement, in this case performed on a Cr-doped PZT-PMN ceramic material [32], [33]. The electrode area (A) was 5x10$^{-4}m^2$. Figure 10(a) shows the raw data of current and temperature versus time. The heating and cooling rates are plotted in Figure 10(b), together with the corresponding pyroelectric currents. There were significant TSC effects in this specimen. Assuming that the TSC is purely a function of temperature, and not time, then the total measured currents (i_m) on heating and on cooling can be described as:

$$i_m^h = p\dot{T}_h A + i_{tsc} \text{ Heating} \tag{13}$$

$$i_m^c = p\dot{T}_c A + i_{tsc} \text{ Cooling} \tag{14}$$

where $\dot{T}$ is the rate of change of temperature with time and i_{tsc} is the magnitude of the thermally stimulated current at any given temperature. The i_{tsc} can be calculated from:

$$i_{tsc} = \frac{\dot{T}_c i_m^h + \dot{T}_h i_m^c}{\dot{T}_c - \dot{T}_h} \tag{15}$$

Once the TSC is known the reversible pyroelectric coefficients can be calculated from equations 13 and 14. These parameters are plotted in Figure 10(c) for this sample. The TSC is small at room temperature (ca 50pA) but quite significant at elevated temperatures (ca 0.2 nA, or 10% of the pyroelectric current.

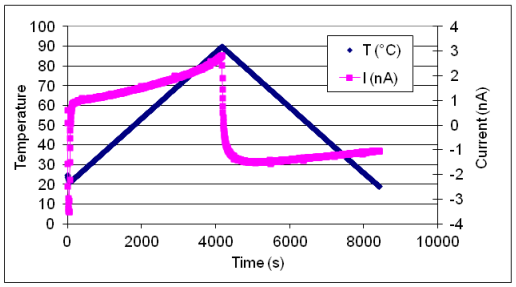

(a)

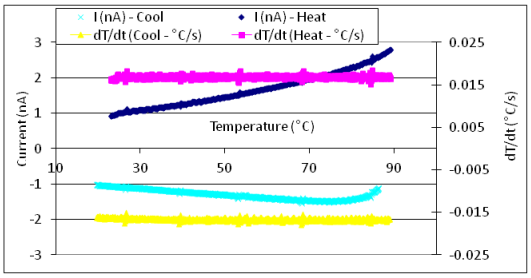

(b)

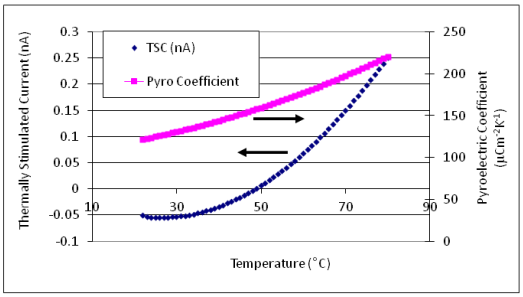

(c)

Fig. 10. (a) Pyroelectric currents measured on heating and cooling a Cr-doped PZT-PMN ceramic material (b) Pyroelectric currents and heating / cooling rates as a function of temperature (c) Calculated TSC magnitude and pyroelectric coefficient as a function of temperature. (Data from [34]).

An alternative method for measuring the pyroelectric current consists of making small sinusoidal temperature oscillations about some average temperature, and measuring the current produced [33], [34], [35], [36]. An example of the results of this kind of measurement are shown in Figure 11(a). Figure 11(b) shows three sinusoidal temperature cycles, and the resulting pyroelectric currents.

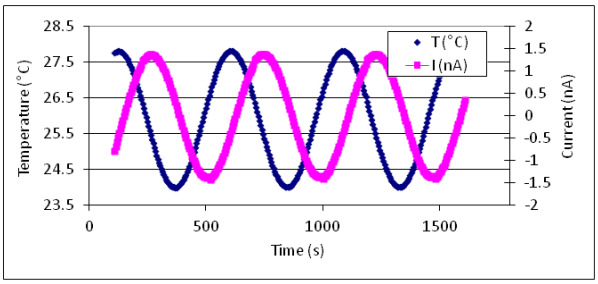

(a)

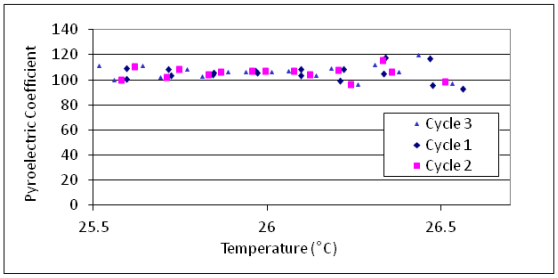

(b)

Fig. 11. Alternative method for pyroelectric properties: a) sinusoidal temperature cycles and measured pyroelectric current and b) calculated pyroelectric coefficient based on the three cycles in a).

The pyroelectric coefficient can be calculated using Equation 16 below [13]:

$$p(T) = \frac{i_{0m}}{\Delta T.A\omega}\sqrt{\left(\frac{R_e}{R_S}+1\right)^2 + \omega^2 R_e^2 C^2} \tag{16}$$

where i_{0m} is the average of the maximum and minimum currents, ω is the angular frequency of temperature oscillation of amplitude ΔT, A is the electrode area, R_e is the resistance of the electrometer (this depends on the instrument

range and can be taken from the electrometer specification), and R_S is the resistance of the sample. The effect of TSC on the current plot would be to give a constant DC offset to the measured current (provided the amplitude ΔT is not too great) and hence this method is not badly affected by this perturbation. The value of R_e for a Keithley 6517 electrometer on a 20nA FSD range would be $<$ 50KW (Ref), so if $R_S = 10^9\Omega$ and $\omega R_e C \ll 1$, the term under the square-root in Equation 16 is very close to unity. For the data shown in Figure 11(a), i_{0m}=2.79nA, ω=0.0132s^{-1} and ΔT =3.81°C, giving $p = 110mCm^{-2}K^{-1}$. This can be checked by calculating the pyroelectric coefficient from the equation $p = i_m/(\dot{T}A)$, point-by-point through the high gradient parts of the cycle. The values are shown in Figure 11(b) for three of the cycles. Close to 26°C (the mid-point of the thermal cycle) it can be seen that all the cycles give a value close to $p = 110mCm^{-2}K^{-1}$. However, the degree of scatter in the measurement increases as the datapoints move away from this temperature.

Irradiation Methods

This method, first described by Chynoweth [37], is related to the technique described at the end of the last section. It involves illuminating the specimen with a sinusoidally-varying-source of infra-red radiation and measuring the resulting pyroelectric current as a consequence of the temperature changes in the material. This is illustrated schematically in Figure 12.

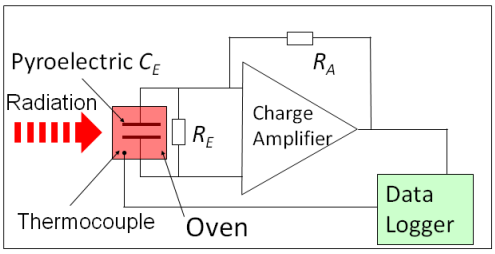

Fig. 12. The "Chynoweth" method for measuring pyroelectric coefficients using AC modulated IR radiation to heat the specimen [37].

The method has the great advantage that the temperature of the specimen is continuously cycled by a small amount (usually a fraction of a degree) about an average temperature, which is close to the operation of a pyroelectric detector. The RMS current signal is usually measured using a lock-in amplifier and is unaffected by DC components such as TSC. The disadvantage of

the method is that the amount of radiation absorbed is dependent upon the emissivity (η) of the front electrode, so that it can be difficult to be certain of the actual temperature change in the specimen. The radiation can be from a hot body (usually held at ca 500K), although some authors have used visible or near-IR radiation (e.g. from a gas or solid state laser) for the same purpose. The rms temperature variation (θ_{rms}) for a sample of thermal mass H with a thermal conductance G_T to a heat-sink, when illuminated by radiation of intensity W, modulated at an angular frequency ω is:

$$\theta_{rms} = \frac{\eta W}{\sqrt{(G^2 + \omega^2 H^2)}} \tag{17}$$

As an example, consider a 1mm square, 50 micron thick piece of a pyroelectric ceramic with $c' = 2.8\text{x}10^6 Jm^{-3}K^{-1}$, bonded to a copper heat sink with a thermal conductance of 1mW/K (typical for a silver epoxy bond). If illuminated with 5mW of radiation, modulated at 10 rad/s with η=0.5, this would give $\theta_{rms} = 1.4°C$ and an rms current response of 11.5nA if the pyroelectric coefficient is $400\mu Cm^{-2}K^{-1}$. This is readily measurable using a commercial current amplifier, but it indicates the importance of having good shielding and keeping the electrical noise to a minimum. Increasing the thickness by a factor 10 (to 0.5mm) would reduce the current output to 1.4nA.

This method relies upon having a good understanding of the operation of the physics of the set-up and the extraction of the basic pyroelectric coefficient from measured pyroelectric current is not straightforward. The 'direct heating' AC method described in the previous section is a much better way to get this parameter. However, the radiation illumination method is a good way to eliminate non-reversible pyroelectric effects and can be a useful method for this reason, if used in conjunction with more direct methods.

Some problems to be aware of with this method:

- If visible radiation is used for illumination, in some cases the results can be complicated by the release of currents due to photoelectric effects.
- The simple theory of pyroelectric devices assumes sinusoidal modulation of the illuminating radiation, so care is required to ensure that the time-waveform of the illuminating radiation is close-to sinusoidal. (This is easy to do with a near-IR solid-state laser, for example). Otherwise, the effects of the higher frequency components of the illuminating waveform must be taken into consideration. In the case of square-wave illumination, the intensity of the higher harmonics can be significant, considerably distorting the frequency response curve from the ideal. For the example given above, if square-wave modulated radiation, then the higher harmonic terms would

boost the apparent response by about 32% relative to a pure sinusoidally-modulated illumination.

4.3 Dielectric Measurements

The measurement of dielectric constant and loss is well-described elsewhere in this book (**??**) and so will not be discussed in detail here, other than to mention the key points which pertain to pyroelectric materials. These are as follows:

- It is essential that the dielectric properties are measured under realistic operating conditions. This means that the frequency range of measurement must be chosen to be relevant to the device application. This is particularly important for measurement of $\tan\delta$, which can be strongly dependent on frequency, especially at low frequencies. Most pyroelectric devices are operated in the range from 0.1Hz (for motion sensors) up to about 100Hz. This poses a problem for many commercial measurement systems (LCR meters and impedance analysers), which are generally designed to work best at high frequencies. Some instruments are specified to low frequencies, however. For example, the Agilent E4980 and Wayne Kerr 6430B are both specified to measure down to 20Hz, which is within the most-relevant range. There is only one commercial instrument which is specified to go below this frequency, the Solartron Frequency Response Analyser, with 1296a Dielectric Interface will measure down to 10μHz.
- The dielectric properties of ferroelectric materials are strongly temperature dependent and must be measured over the range of temperatures that the device is to be operated over.
- The dielectric properties of single crystals must be measured for a minimum of three different crystal cuts if the full dielectric constant tensor is to be specified. This is important, as the figure of merit p/ϵ can be optimised for a crystal cut which is not perpendicular to the major axis for the p vector. This was first shown by Shaulov to be the case for deuterated triglycine sulphate crystals [38].

Electrical Resistivity

The bias resistor R_G in Figure 4 performs an important function in the circuit, in that it both sets the electrical time constant and also biases the gate of the FET. For single element detectors, it is possible to include this as an explicit circuit element, in which case a very high value component is needed (ca $10^{12}\Omega$ for a 10s time constant with C=10pF). However, such components are expensive. For large arrays, it is impossible to include a separate resistor for each element. In this case, it is desirable to be able to use the intrinsic DC resistivity (ρ) of the element to provide the required resistance. In this case,

we can set the electrical time constant from $\tau_e = \rho\epsilon\epsilon_0$, so that for a ceramic with ϵ=300, we need ρ = 4x$10^9\Omega m$. There are thus two issues to address. The first is the best method for measuring the DC resistivity in the range 10^8 to $10^{12}\Omega m$. The second is the method for controlling it. While many excellent commercial electrometers are available that will permit the accurate measurement of high resistances, the accurate measurement of very high DC resistivities is not trivial. Surface moisture is a major problem and the measurements should ideally be carried out under vacuum, after heating the specimen to expel any adsorbed moisture from the surface. For the most-accurate measurements, guard-ring methods should be used. A further consideration in the measurement of resistivity is the relaxation time associated with the polarisation of immobile charges in the material. This is particularly important for materials that have only moderately-high resistivities. It leads to a peak in current immediately after applying the DC test voltage, followed by an exponential decay in the current to a stable value. The time constant of this decay can be many minutes long and the best way to get the 'DC' value of the resistivity is to measure the current as a function of time and fit it to an equation of the form $i(t) = i_0 \exp 1/t$ where *i(t)* is the current at time t and i_0 is the current at infinite time. The values of i_0 can be obtained by extrapolation of *ln(i(t))* vs *1/t* and used to compute the DC resistivities at 'infinite' time.

Thermal Properties

As noted above, it is important to have a good knowledge of the volume specific heat and the thermal conductivity / thermal diffusivity. There are many excellent differential scanning calorimeter systems available which can be used to measure the specific heat which, when combined with the sample density can be used to give c'. The thermal diffusivity (which can be important for thermal imaging systems if the target is not reticulated) can be measured directly on a pyroelectric substrate using the laser intensity modulation method (LIMM) described by Lang [39], [40], [41] or by using a flash illumination technique [42].

Piezoelectric coefficients

The techniques used for measurement of piezoelectric properties on bulk materials and thin films are described elsewhere in this book. As noted above, the key coefficients to measure for pyroelectric applications are d_{31} and e_{31}, so that they can be used to model the effects of piezoelectric microphony and the generation of secondary pyroelectric effects due to substrate clamping and thermal expansion effects.

5 Examples of pyroelectric materials

There are many different types of pyroelectric, including single crystals, polymers, ceramics and thin films and several reviews [1], [16], [20] have considered the properties of many pyroelectric materials in detail, so the discussion here has been confined to a brief review of pyroelectric ceramics and thin films.

6 Conclusions

This chapter has provided a review of the physics of pyroelectric radiation detectors, the critical physical properties which determine their performance and the various techniques for measuring these. Considerable care is needed, and it is especially important to consider the way in which the material is to be used in the ultimate application the measurement methodologies to be used are selected. This applies especially to the measurement frequencies used for the dielectric properties, which can have a dramatic effect on the results, especially for dielectric loss.

References

1. R. W. Whatmore, "Pyroelectric devices and materials," *Reports on Progress in Physics*, vol. 49, no. 12, p. 1335, 1986.
2. R. W. Whatmore and R. Watton, "Pyroelectric Materials and Devices." in *"Infrared Detectors and Emitters: Materials and Devices"*, P. Capper and C. T. Elliott, Eds. Kluwer Academic Publishers, The Netherlands, 1998, pp. 99–148.
3. R. C. Evans, *An Introduction to Crystal Chemistry.* Cambridge University Press, 1964.
4. S. Kasap and P. Capper, *R.W. Whatmore, Ferroelectric Materials pp597-623 in Springer Handbook of Electronic and Photonic Materials*, ser. Springer handbooks. Springer, 2006.
5. J. F. Nye, *Physical Properties of Crystals: Their Representation by Tensors and Matrices*, ser. Oxford science publications. Clarendon Press, 1985.
6. W. Pontes, A. A. d. Carvalho, W. K. Sakamoto, M. H. d. Paula, M. A. A. Sanches, R. L. B. de Freitas, R. B. P. César, and S. L. Piubéli, "PZT FOR MEASURING ENERGY FLUENCE RATE OF X-RAY USED IN SUPERFICIAL CANCER THERAPY," *Instrumentation Science & Technology*, vol. 38, no. 3, pp. 210–219, Apr. 2010.
7. T. M. Lee, A. P. Anderson, and F. A. Benson, "Microwave field-detecting element based on pyroelectric effect in PVDF," *Electronics Letters*, vol. 22, no. 4, pp. 200–202, 1986.
8. P. W. Kruse, "Uncooled IR focal plane arrays," *SPIE's 1995 International Symposium on Optical Science, Engineering, and Instrumentation*, vol. 2552, pp. 556–563, 1995.
9. N. Nelms and J. Dowson, "Goldblack coating for thermal infrared detectors," *Sensors and Actuators A: Physical*, vol. 120, no. 2, pp. 403–407, May 2005.

10. W. Lang, K. Kühl, and H. Sandmaier, "Absorbing layers for thermal infrared detectors," *Sensors and Actuators A: Physical*, vol. 34, no. 3, pp. 243–248, 1992.
11. A. D. Parsons, "Thin-film infrared absorber structures for advanced thermal detectors," *Journal of Vacuum Science & Technology A: Vacuum, Surfaces, and Films*, vol. 6, no. 3, p. 1686, May 1988.
12. J. H. Lehman, C. Engtrakul, T. Gennett, and A. C. Dillon, "Single-wall carbon nanotube coating on a pyroelectric detector," *Applied optics*, vol. 44, no. 4, pp. 483–488, 2005.
13. M. Yun, J. Bock, H. Leduc, P. Day, and M. J. Kim, "Fabrication of antenna-coupled transition edge polarization-sensitive bolometer arrays," *Nuclear Inst. and Methods in Physics Research, A*, vol. 520, no. 1–3, pp. 487–489, 2004.
14. D. H. Auston and A. M. Glass, "Optical Generation of Intense Picosecond Electrical Pulses," *Applied Physics Letters*, vol. 20, no. 10, p. 398, 1972.
15. V. Blackmore, G. Doucas, C. Perry, B. Ottewell, M. Kimmitt, M. Woods, S. Molloy, and R. Arnold, "First measurements of the longitudinal bunch profile of a 28.5 GeV beam using coherent Smith-Purcell radiation," *Physical Review Special Topics - Accelerators and Beams*, vol. 12, no. 3, p. 032803, Mar. 2009.
16. P. Capper and C. T. Elliott, *Infrared Detectors and Emitters: Materials and Devices*, ser. Electronic materials series. Kluwer Academic, 2001.
17. R. K. Willardson and A. C. Beer, *E.H. Putley (1970), The pyroelectric detector, in SEMICONDUCTORS and SEMIMETALS*. Elsevier Science, 1970.
18. E. H. Putley, "A method for evaluating the performance of pyroelectric detectors," *Infrared Physics*, vol. 20, no. 3, pp. 139–147, 1980.
19. H. H. S. Chang, R. W. Whatmore, and Z. Huang, "Pyroelectric effect enhancement in laminate composites under short circuit condition," *Journal of Applied Physics*, vol. 106, no. 11, p. 114110, 2009.
20. P. Muralt, "Micromachined infrared detectors based on pyroelectric thin films," *Reports on Progress in Physics*, vol. 64, no. 10, p. 1339, 2001.
21. N. M. Shorrocks, R. W. Whatmore, M. K. Robinson, and S. G. Porter, "Low microphony pyroelectric arrays," *Proc. SPIE (1985) 588 44-51*, pp. 44–51, 1986.
22. A. J. Bell and R. W. Whatmore, "Electrical conductivity in uranium doped, modified lead zirconate pyroelectric ceramics," *Ferroelectrics*, vol. 37, no. 1, pp. 543–546, 1981.
23. R. W. Whatmore, "High performance, conducting pyroelectric ceramics," *Ferroelectrics*, vol. 49, no. 1, pp. 201–210, 1983.
24. S. B. Stringfellow, S. Gupta, C. Shaw, J. R. Alcock, and R. W. Whatmore, "Electrical conductivity control in uranium-doped PbZrO3-PbTiO3-Pb (Mg1/3Nb2/3) O3 pyroelectric ceramics," *Journal of the European Ceramic Society*, vol. 22, no. 4, pp. 573–578, 2002.
25. R. W. Whatmore and A. J. Bell, "Pyroelectric ceramics in the lead zirconate-lead titanate-lead iron niobate system," *Ferroelectrics*, vol. 35, no. 1, pp. 155–160, 1981.
26. J. M. Herbert, *Ferroelectric transducers and sensors*, ser. Electrocomponent science monographs. Gordon and Breach Science Publishers, 1982.
27. A. Kumar and M. M. Periman, "Simultaneous stretching and corona poling of PVDF and P (VDF-TriFE) films. II," *Journal of Physics D: Applied Physics*, vol. 26, no. 3, p. 469, 1993.
28. J. M. Marshall, Q. Zhang, and R. W. Whatmore, "Corona poling of highly (001)/(100)-oriented lead zirconate titanate thin films," *Thin Solid Films*, vol. 516, no. 15, pp. 4679–4684, Jun. 2008.

29. S. B. Lang and F. Steckel, "Method for the Measurement of the Pyroelectric Coefficient, dc Dielectric Constant, and Volume Resistivity of a Polar Material," *Review of Scientific Instruments*, vol. 36, no. 7, p. 929, 1965.
30. A. M. Glass, "Investigation of the Electrical Properties of Sr1xBaxNb2O6 with Special Reference to Pyroelectric Detection," *Journal of Applied Physics*, vol. 40, no. 12, p. 4699, 1969.
31. R. L. Byer and C. B. Roundy, "Pyroelectric coefficient direct measurement technique and application to a nsec response time detector," *Ferroelectrics*, vol. 3, no. 1, pp. 333–338, 1972.
32. R. W. Whatmore, O. Molter, and C. P. Shaw, "Electrical properties of Sb and Cr-doped PbZrO 3–PbTiO 3–PbMg 1/3 Nb 2/3 O 3 ceramics," *Journal of the European Ceramic Society*, vol. 23, no. 5, pp. 721–728, 2003.
33. O. Molter, "Development of new pyroelectric ceramics for thermal imaging applications / Olivier Molter." Ph.D. dissertation, Thesis (M.Sc.) - Cranfield University, School of Industrial and Manufacturing Science, Advanced Materials, 2001., Cranfield University, 2001.
34. R. W. Whatmore, O. Molter, and C. Shaw, "Electrical properties of Sb and Cr-doped PbZrO 3–PbTiO 3–PbMg 1/3 Nb 2/3 O 3 ceramics," *Journal of the European Ceramic Society*, vol. 23, no. 5, pp. 721–728, 2003.
35. E. J. Sharp and L. E. Garn, "Use of low-frequency sinusoidal temperature waves to separate pyroelectric currents from nonpyroelectric currents. Part II. Experiment," *Journal of Applied Physics*, vol. 53, no. 12, p. 8980, 1982.
36. L. E. Garn and E. J. Sharp, "Use of low-frequency sinusoidal temperature waves to separate pyroelectric currents from nonpyroelectric currents. Part I. Theory," *Journal of Applied Physics*, vol. 53, no. 12, p. 8974, 1982.
37. A. G. Chynoweth, "Dynamic Method for Measuring the Pyroelectric Effect with Special Reference to Barium Titanate," *Journal of Applied Physics*, vol. 27, no. 1, p. 78, 1956.
38. A. Shaulov, "Improved figure of merit in obliquely cut pyroelectric crystals," *Applied Physics Letters*, vol. 39, no. 2, p. 180, 1981.
39. S. B. Lang, "Laser intensity modulation method: A technique for determination of spatial distributions of polarization and space charge in ferroelectric materials," *Ferroelectrics*, vol. 78, no. 1, pp. 129–136, 1988.
40. S. Lang, "Technique for the measurement of thermal diffusivity based on the laser intensity modulation method (LIMM)," *Ferroelectrics*, vol. 93, no. 1, pp. 87–93, 1989.
41. M. Stewart and M. G. Cain, "Spatial Characterization of Piezoelectric Materials Using the Scanning Laser Intensity Modulation Method (LIMM)," *Journal of the American Ceramic Society*, vol. 91, no. 7, pp. 2176–2181, Jul. 2008.
42. W. J. Parker, R. J. Jenkins, C. P. Butler, and G. L. Abbott, "Flash Method of Determining Thermal Diffusivity, Heat Capacity, and Thermal Conductivity," *Journal of Applied Physics*, vol. 32, no. 9, p. 1679, 1961.